

Photoresponse in $\text{La}_{0.9}\text{Hf}_{0.1}\text{MnO}_3/0.05\text{wt}\%\text{Nb}$ -doped SrTiO_3 heteroepitaxial junctions

Yaping Qi,^{1,a} Hao Ni,^{1,3} Ming Zheng,¹ Jiali Zeng,¹ Yucheng Jiang,^{2,a}
and Ju Gao^{1,2,a}

¹Department of physics, Chong Yuet Ming Physics Building, The University of Hong Kong, Pokfulam Road, Hong Kong

²Jiangsu Engineering Laboratory for Bio-sensor and chip technology, Jiangsu Key Laboratory of Micro-Nano Heat Fluid Flow Technology and Energy Application, School of Mathematics and Physics, Suzhou University of Science and Technology, Suzhou, Jiangsu 215009, PR China

³College of Science, China University of Petroleum, Qingdao 266580, China

(Presented 10 November 2017; received 8 September 2017; accepted 25 October 2017; published online 12 December 2017)

Excellent photo detectors need to have the rapid response and good repeatability from the requirement of industrial applications. In this paper, transport behavior and opto-response of heterostructures made with $\text{La}_{0.9}\text{Hf}_{0.1}\text{MnO}_3$ and 0.05wt%Nb-doped SrTiO_3 were investigated. The heterojunctions exhibited an excellent rectifying feature with very low leakage in a broad temperature region (from 40 to 300 K). These thin films presented persistent and stable photovoltages upon light illumination. Rapid shift between small and large voltages corresponding to “light OFF” and “light ON” states, respectively, was observed, demonstrating reliable photo detection behavior. A semiconductor laser with a wavelength of 650 nm was used as the light source. It is also noted that the observed photovoltages are strongly determined by light intensity. The injection of photoexcited charge carriers (electrons) could be responsible for the appearance of the observed opto-response. Such manipulative features by light irradiation exhibit great potential for light detectors for visible light. © 2017 Author(s). All article content, except where otherwise noted, is licensed under a Creative Commons Attribution (CC BY) license (<http://creativecommons.org/licenses/by/4.0/>). <https://doi.org/10.1063/1.5003914>

I. INTRODUCTION

There are numerous studies on perovskite-type oxides due to their attractive and complex properties. Heterojunctions composed of different oxides may even exhibit potential in different products, such as photo detection, diodes, solar cells, electric devices, and so on.¹⁻⁴ Therefore, perovskite oxide heterojunctions have been extensively investigated over the last decades. Because of good lattice match, niobium doped SrTiO_3 (NSTO) is widely used as the substrate for perovskite oxides. Heterostructures composed of (doped) strontium titanate (SrTiO_3) and manganites have been intensively studied. Partially substituting Ti with Nb makes STO become n -type semiconductor. Previous studies demonstrated that $\text{La}_{0.9}\text{Hf}_{0.1}\text{MnO}_3$ (LHMO) was electron-doped manganite as a reliable n -type semiconductor.^{5,6} Heterojunctions composed of NSTO and manganite showed some fascinating characteristics in comparison to the conventional semiconductor n - n junctions.⁷

The magnetic and electronic properties of manganese is highly sensitive to strain, current, electric field, magnetic fields and photo illumination,⁸⁻¹² these extraordinary properties make these simple n - n junctions promising for practical application in the near future. The complicated interactions amongst their charges, spin, orbital and lattice degree of freedom cause many interesting and phenomena.

^aE-mail: joyceqi@connect.hku.hk, jyc@usts.edu.cn, jugao@hku.hk

The response of manganite to lights with various wavelengths and energy densities have attracted much attention recently. Various techniques have been used to identify the light-induced effects. J. R. Sun et al. studied photovoltaic effect of heterojunctions composed of $\text{La}_{0.7}\text{Ce}_{0.3}\text{MnO}_3$ and NSTO (001).¹³⁻¹⁵ Photo-induced effect have been report in $\text{La}_{0.67}\text{Ca}_{0.33}\text{MnO}_3/\text{Si}$, $\text{LHMO}/\text{STO}/\text{Si}$, $\text{La}_{0.1}\text{Sr}_{0.9}\text{MnO}_3/\text{NSTO}$ and $\text{La}_{0.8}\text{Hf}_{0.2}\text{MnO}_3/0.7\text{wt}\% \text{Nb-SrTiO}_3$ heterojunctions.^{3,4,12,16}

In this study, LHMO and 0.05wt%Nb-doped SrTiO_3 (0.05wt%Nb-STO) thin films have been designed, and their structures, transport properties and optical properties have been systemically investigated for light detectors for visible light.

II. EXPERIMENTAL

Epitaxial LHMO films were prepared onto (001)-oriented 0.05wt%Nb-STO single-crystal substrate using pulsed laser deposition.¹⁷ The deposition was carried out under 2 Pa oxygen pressure at 700 °C.¹⁸ To enhance crystallinity quality and to reduce possible oxygen deficiencies, LHMO films were *in situ* annealed in 1.5×10^3 Pa high-purity O_2 at 700 °C for 2 hours.¹⁹ The thickness of LHMO films was approximately 40 nm measured by transmission electron microscopy (TEM) and step profiler. The ohmic contacts were achieved using silver electrodes, which were deposited by thermal evaporation.²⁰ Transport properties and photoelectric effects were measured using traditional two-probe method at various temperatures by a Superconducting Quantum Interference Device (SQUID). Semiconductor lasers with wavelength of 650 nm with variable power densities were applied to investigate the photo-induced effects.

III. RESULTS AND DISCUSSION

The as grown samples were examined by XRD (SIEMENS D5000 with $\text{Cu-K}\alpha$ radiation) θ - 2θ scan profile. For all LHMO films on 0.05wt%Nb-STO, there are strong overlaps of reflection peaks for LHMO and 0.05wt%Nb-STO as shown in Figure 1. This is because the lattice parameter of bulk LHMO ($a_{\text{LHMOps}} \sim 3.894 \text{ \AA}$) is very close to that of 0.05wt%Nb-STO ($a_{\text{NSTO}} \sim 3.905 \text{ \AA}$).²¹ No extra peaks other than (001) peaks of LHMO and 0.05wt%Nb-STO could be found from the graph, this indicated that the LHMO films grow along c-axis orientation and are of single phase. The insert of Figure 1 presents the schematic diagram of the heterojunctions composed of LHMO and 0.05wt%Nb-STO.

Figure 2 demonstrated the relationship between the current versus the voltage. Compared with most other reports on manganite-based heterojunctions, the heterojunctions composed of LHMO and

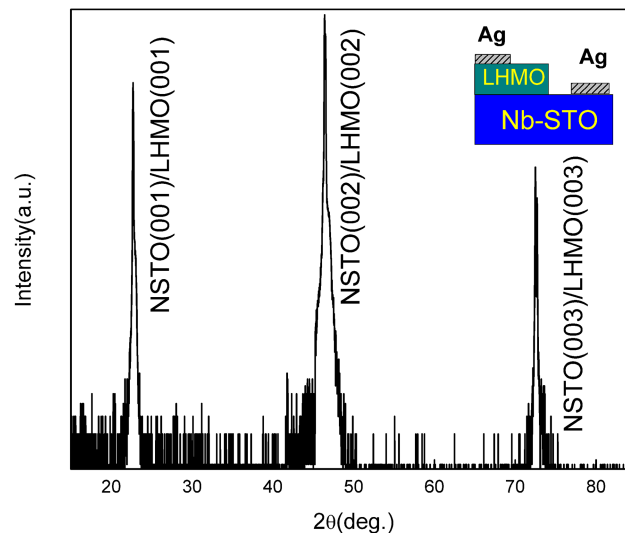


FIG. 1. XRD pattern (θ - 2θ scan) of $\text{La}_{0.9}\text{Hf}_{0.1}\text{MnO}_3/0.05\text{wt}\% \text{Nb-doped SrTiO}_3$. The insert is schematic view of the junction.

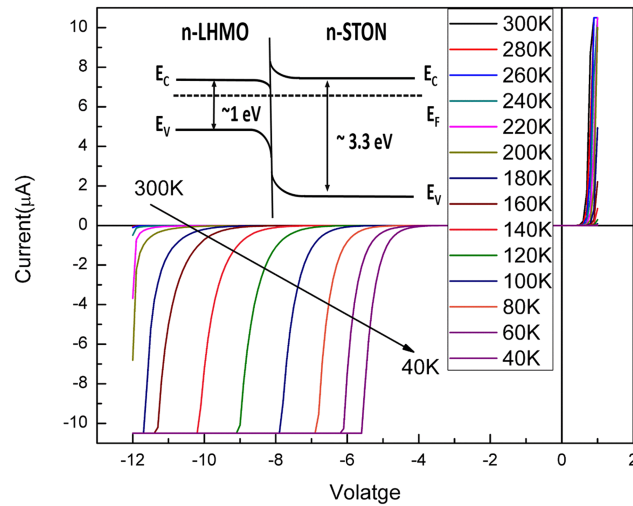


FIG. 2. Rectifying characteristics of $\text{La}_{0.9}\text{Hf}_{0.1}\text{MnO}_3/0.05\text{wt}\%\text{Nb}$ -doped SrTiO_3 heterostructures in a wide temperature range (from 40 to 300K), the insert is schematic energy band diagram for $\text{La}_{0.9}\text{Hf}_{0.1}\text{MnO}_3/0.05\text{wt}\%\text{Nb}$ -doped SrTiO_3 heterojunction.

0.05wt%Nb-STO showed more obviously asymmetry of I-V relationship. They exhibited excellent rectifying properties with small leakage current in a broad temperature region from 40 K to 300 K, which are comparable with those *p-n* junctions made of classic semiconductors. A clear asymmetry for positive and negative bias was noticed (Figure 2). Although the comprehensive transport mechanism is still uncertain for manganite-based junctions, previous studies indicated that the I-V characteristics for these heterojunctions could be considered using *p-n* junction or Schottky junction models.^{22,23} It is widely believed that this might be caused by the energy band diagram of LHMO and 0.05wt%Nb-STO heterostructures, as shown in the inset of Figure 2. The energy barrier could be obtained between the interface of LHMO and 0.05wt%Nb-STO. It would be decreased at the positive direction. When the positive bias is bigger than the energy barrier, electrons would transfer from the conduction band of 0.05wt%Nb-STO to conduction band of LHMO. This results in the rapid rise of current. However, at the negative bias, the energy barrier could be increased, resulting in forbiddance of the electron transition between the conduction band of 0.05wt%Nb-STO and LHMO. Thus, the electrons in the valance band of LHMO could only be transferred into the conduction band of 0.05wt%Nb-STO when the negative bias is large enough. Compared with our previous reports on $\text{La}_{0.8}\text{Hf}_{0.2}\text{MnO}_3/0.7\text{wt}\%\text{Nb}$ -STO heterostructures, one significant difference was that a higher leakage current occurred at high temperature in LHMO/0.05wt%Nb-STO junctions. According to the reference, it is suggested that strain and different phase of LHMO were attributed to such a phenomenon.^{8,16,24}

To examine the microstructural features of this heterostructure, a typical sample was examined by TEM. The results of TEM were shown in Figure 3. It demonstrated the excellent epitaxial growth of LHMO layer. In Figure 3(a), a clear interface of the LHMO/0.05wt%Nb-STO heterojunctions

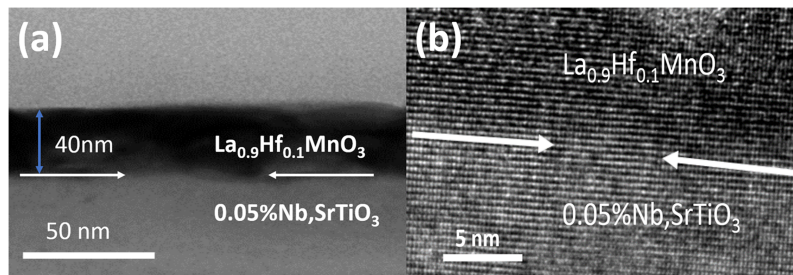


FIG. 3. (a) Cross-sectional TEM image of $\text{La}_{0.9}\text{Hf}_{0.1}\text{MnO}_3/0.05\text{wt}\%\text{Nb}$ -doped SrTiO_3 (b) HRTEM image of the interface of $\text{La}_{0.9}\text{Hf}_{0.1}\text{MnO}_3/0.05\text{wt}\%\text{Nb}$ -doped SrTiO_3 .

was noted. The thickness of LHMO film was about 40 nm. High resolution TEM patterns of each interface are shown in Figure 3(b). It displayed the atoms in LHMO Layer are quite distinct and with high order. The interface was very sharp and clear. No obvious atomic inner diffusion was observed with the adjacent materials.

In order to view these heterojunctions composed of LHMO and 0.05wt%Nb-STO for the potential applications in optoelectronic detection devices, the relationship between heterojunction voltage and illumination time was investigated under light illumination ($\lambda=650$ nm) at different power densities of laser at 300 K (Figure 4).

In the beginning, the temporal recovery of electric conductivity of this heterojunction was explored at 300 K. To test this, a laser with wavelength of 650 nm was illuminated perpendicularly on the surface of these thin films, and the power density were 15, 10, 5, 2 and 1 mw/cm^2 respectively. To start this experiment, the laser was turned on firstly then it was turned off after several minutes. The results were shown in Figure 4(a), and showed how photovoltage behave with the changing of time. The voltages abruptly increased by exposure to light. After 1700 seconds,

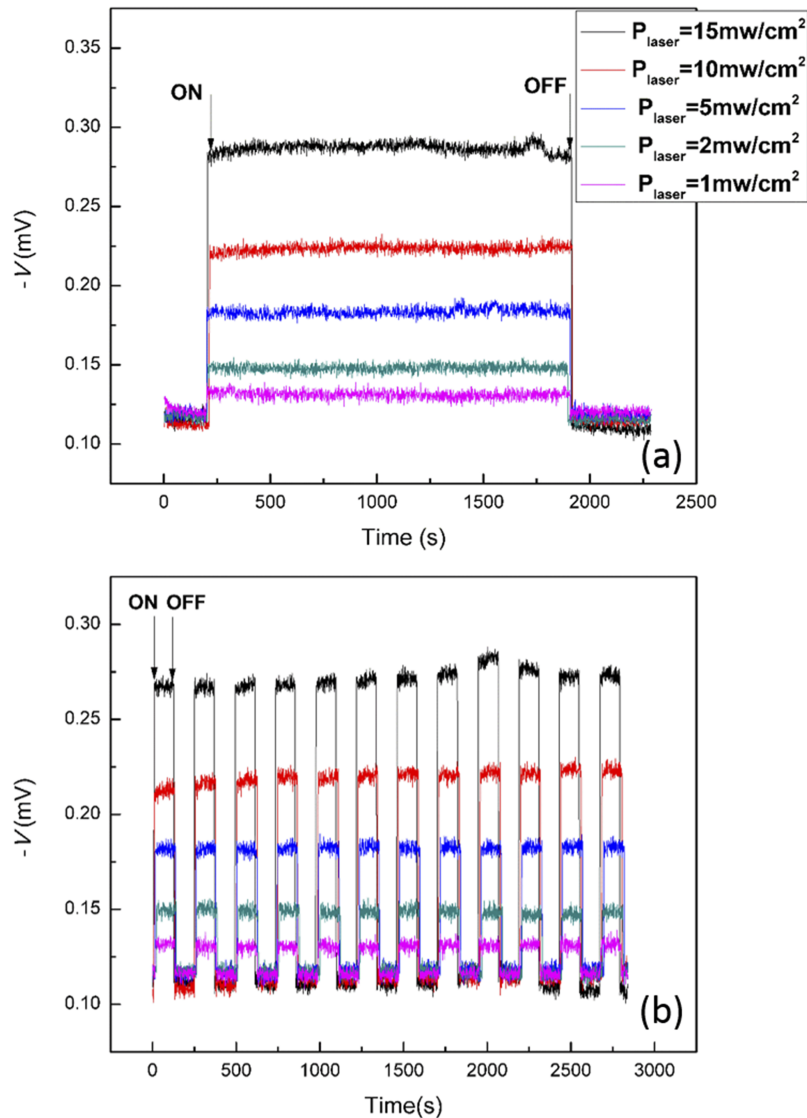


FIG. 4. Figure illustrating (a) The relationship between voltage and illumination time for $\text{La}_{0.9}\text{Hf}_{0.1}\text{MnO}_3/0.05\text{wt}\%\text{Nb}$ -doped SrTiO_3 heterojunctions, showing persistent photocurrent (b) Response of photovoltage to the intermittent light irradiation (sampling current: $-1 \mu\text{A}$; Wavelength: 650 nm; power densities: 1, 2, 5, 10 and 15 mw/cm^2 ; temperature: 300 K).

the persistent photovoltage stabilized at a high level. Then the illumination was switched off, but the voltages almost recovered to the initial stage immediately. It was also found that with the increase of photon energy of incident light from 1 to 15 mw/cm², the change of photovoltage become more and more distinct. Figure 4(b) demonstrated the photovoltage responses for twelve cycles. It presented quick switch between small and large voltages corresponding to “light OFF” and “light ON” states, respectively, suggesting LHMO/0.05wt%Nb-STO heterojunctions to be nice photo detectors due to persistent and stable photovoltages observation.

The rectifying I–V and photoelectric characteristic of the junctions usually originate from the energy band bending. For references,^{25,26} the energy gaps of LHMO and 0.05wt%Nb-STO are approximately 1 and 3.2 eV, respectively; and the electron affinity of LHMO and 0.05wt%Nb-STO are approximately 4.1 and 4 eV, respectively. The Fermi level of LHMO is supposed to be close to the bottom of the conduction band due to an *n*-type semiconductor LHMO. Since the photon energy of 650 nm wavelength (1.91 eV) is larger than the bandgap of LHMO and smaller than that of 0.05wt%Nb-STO, nonequilibrium electron-hole pairs can only generated in the LHMO layer. Under light illumination, holes and electrons are created in the valence and conduction bands of LHMO layer, respectively. Among them, electrons can be transferred to the 0.05wt%Nb-STO across the interface, whereas holes cannot cross the interface due to the large barrier. As a result, photo excited holes and electrons are spatially separated, leading to the appearance of the photovoltage.

IV. CONCLUSIONS

In summary, heterojunctions of LHMO/0.05wt%Nb-STO were fabricated by PLD method. XRD spectra demonstrated a good epitaxy and crystallinity. The heterojunctions showed excellent rectifying properties in a wide temperature range, which is comparable with those *p-n* junctions made of traditional semiconductors. Photo-induced voltage was also observed as illuminated by visible light. It was found that the observed photovoltage strongly depends on the light intensity. Opto-response of these junctions and transport behavior are tunable. These results revealed the feasible manipulation of electrical transport of LHMO/0.05wt%Nb-STO junctions by light irradiation, and suggested that these junctions can be good optoelectronic devices based on manganite perovskites. According to the mechanism of photovoltage in the LHMO/0.05wt%Nb-STO structure, whose energy is larger than the bandgap of LHMO, LHMO/0.05wt%Nb-STO has the potential to be a good detector for visible and ultraviolet lights.

ACKNOWLEDGMENTS

This work has been supported by the National Key Project for Basic Research (No. 2014CB921002), the National Natural Science Foundation of China (Grant No. 11374225, 11574227, 11504432), and the Research Grant Council of Hong Kong (Project No. HKU701813). It is also supported by PAPD, USTS Cooperative Innovation Center, and Suzhou Key Laboratory for Low Dimensional Optoelectronic Materials and Devices (SZS201611).

¹ D. S. Shang *et al.*, *Appl. Phys. Lett.* **93**, 172119 (2008).

² H. B. Lu *et al.*, *Appl. Phys. Lett.* **86**, 032502 (2005).

³ J. Du *et al.*, *Opt. Express* **19**, 17260 (2011).

⁴ X. B. Liu, L. B. Jin, H. B. Lu, and J. Gao, *Appl. Phys. Lett.* **108**, 173502 (2016).

⁵ L. Wang and J. Gao, *J. Appl. Phys.* **105**, 07C904 (2009).

⁶ L. Wang and J. Gao, *J. Appl. Phys.* **105**, 07E514 (2009).

⁷ F. X. Hao *et al.*, *Appl. Phys. Lett.* **109**, 131104 (2016).

⁸ E. J. Guo *et al.*, *J. Appl. Phys.* **110**, 113914 (2011).

⁹ A. Congeduti *et al.*, *Rev. Lett.* **86**, 1251 (2001).

¹⁰ H. B. Lu *et al.*, *Appl. Phys. Lett.* **86**, 032502 (2005).

¹¹ J. M. Dai *et al.*, *J. Appl. Phys.* **90**, 3118 (2001).

¹² Z. Luo and J. Gao, *J. Appl. Phys.* **100**, 056104 (2006).

¹³ J. R. Sun, C. M. Li, and H. K. Wong, *Appl. Phys. Lett.* **84**, 4804 (2004).

¹⁴ Z. G. Sheng, B. C. Zhao, W. H. Song, Y. P. Sun, J. R. Sun, and B. G. Shen, *Appl. Phys. Lett.* **87**, 242501 (2005).

¹⁵ J. R. Sun *et al.*, *Appl. Phys. Lett.* **87**, 202502 (2005).

¹⁶ Z. P. Wu, L. Wang, and J. Gao, *J. Appl. Phys.* **111**, 07D723 (2012).

- ¹⁷ J. Gao, B. B. G. Klopman, W. A. M. Aarnink, A. E. Reitsma, G. J. Gerritsma, and H. Rogalla, *J. Appl. Phys.* **71**, 2333 (1992).
- ¹⁸ J. Gao, W. H. Wong, and J. Xhie, *Appl. Phys. Lett.* **67**, 2232 (1995).
- ¹⁹ Y. P. Qi *et al.*, *Int. J. Mod. Phys. B.* **31**, 1745022 (2017).
- ²⁰ X. S. Wu, and J. Gao, *Physica. C. Supercond.* **215**, 315 (1999).
- ²¹ L. Wang and J. Gao, *J. Appl. Phys.* **103**, 07F702 (2008).
- ²² T. Susaki, N. Nakagawa, and H. Y. Hwang, *Phys. Rev. B* **75**, 104409 (2007).
- ²³ A. Ruotolo, C. Y. Lam, W. F. Cheng, K. H. Wong, and C. W. Leung, *Phys. Rev. B.* **76**, 075122 (2007).
- ²⁴ J. F. Wang, Y. C. Jiang, M. G. Chen, and J. Gao, *Appl. Phys. Lett.* **103**, 252103 (2013).
- ²⁵ S. M. Guo, Y. G. Zhao, C. M. Xiong, and P. L. Lang, *Appl. Phys. Lett.* **89**, 223506 (2006).
- ²⁶ J. M. D. Coey, M. Viret, and S. Von Molnar, *Adv. Phys.* **48**, 167 (1999).